metals

MDPI

Article

Spark Plasma Sintering and Characterization of Al-TiB_2 Composites

A. Raja Annamalai [1,†], Muthe Srikanth [2,†], A. Muthuchamy [3], Shashank Acharya [2], Anup Khisti [2], Dinesh K. Agrawal [4] and Chun-Ping Jen [5,*]

1 Centre for Innovative Manufacturing Research, VIT, Vellore 632014, India; raja.annamalai@vit.ac.in
2 School of Mechanical Engineering, VIT, Vellore 632014, India; muthe.srikanth@vit.ac.in (M.S.); achashash99@gmail.com (S.A.); anupkhisti96@gmail.com (A.K.)
3 Department of Metallurgical and Materials Engineering, NIT Tiruchirappalli, Tiruchirappalli 620015, India; muthuchamy@nitt.edu
4 Material Research Institute, Pennsylvania State University, State College, PA 16802, USA; dxa4@psu.edu
5 Department of Mechanical Engineering, National Chung Cheng University, Chia-Yi 621, Taiwan
* Correspondence: imecpj@ccu.edu.tw; Tel.: +886-5272-9382
† Equally contributed as 1st author.

Received: 15 July 2020; Accepted: 17 August 2020; Published: 19 August 2020

Abstract: In this study, Al-TiB_2 compacts fabricated by spark plasma sintering methods at different temperatures were characterized for densification, microstructural development, and mechanical properties. Sintering parameters used were temperatures of 500 °C and 550 °C under the pressure of 30 MPa. A very dense microstructure with uniform phase distribution and porosity was produced in the sample sintered at 550 °C with 2.5 wt% TiB_2. The same sample exhibited excellent hardness value, and a high-tensile strength attributed to full metallurgical bonding, presence of sub-micron sized grains, and their uniform distribution. These results show that the TiB_2 addition enhanced the composite's hardness, sintered density, and tensile strength. In all the sintered samples, the fractographs revealed a mixed-mode fracture (ductile and brittle).

Keywords: aluminum alloy; metal matrix composites (MMCs); Al-6061TiB_2; spark plasma sintering; characterization; microstructure

1. Introduction

In the past few decades, metal matrix composites (MMCs) have been extensively used in aviation and automobile industries and defense sectors due to their high toughness, excellent specific strength, and elastic modulus [1]. The properties of MMCs can be enhanced by adding particulate reinforcements [2–4]. Aluminum is one of the low-cost and lightweight metals, and the Al-6061 alloy mainly contains magnesium and silicon. Al-6061 is broadly used in multiple engineering applications, experimentation, and commercial applications including frames of light mobility vehicles, construction, aviation and aerospace, etc. because of its corrosion resistance, superior machinability, good surface finish, etc. Its excellent corrosion resistance makes it an appropriate material for marine structural applications [5]. Various causes such as thermal expansion difference, even distribution of reinforcements, and fabrication conditions that distress the mechanical properties have been examined previously [6–8]. MMCs strengthened by ceramic fibers, whiskers, and particles are most widely used, which possess the ability to strengthen the performance parameters of manufacturing operations. Ceramic particles have high strength, hardness, low thermal expansion, and high chemical resistance. Reinforcements like $ZrSiO_4$, B_4C, TiB_2, and SiC are used to ameliorate the hardness and wear resistance of MMCs without considerably changing the density of the material [9–16]. Among these,

TiB_2 has emerged as a good reinforcement due to its outstanding features such as thermal stability, oxidation resistance, high melting point (3225 °C), and exceptional hardness (25–35 GPa Vickers at room temperature). It is chemically stable for a wide range of temperatures, high modulus, and has good electrical conductivity [17]. Thus, the properties of Al-6061 alloys are greatly improved with the addition of TiB_2 particles [18]. Rana Pratap Singh et al. reported that improved the mechanical properties of Al 2014 with the addition of 5%TiB_2, is fabricated using a powder metallurgy process [19]. Z. Sadeghian et al. stated that Al 20 wt% TiB_2 spark plasma sintered and hot extrude composites have excellent mechanical properties [20]. Another study was done by M. Askarpour et al. using the accumulative roll bonding (ARB) method on Al-TiB_2 composites and reported that the composite had an ultra-high strength and fine grain size [18]. Using a two-step milling method, the Al-TiB_2 nanocomposite was produced [21]. Al-TiB_2 composites are mainly fabricated by stir casting [22] and other different processing techniques are using like friction stir processing [23], salt metal reaction process [24], aluminothermic reaction process [25], etc. to overcome the problems and increase the properties other manufacturing processes are using. Unconventional sintering techniques like pressure less sintering, microwave-assisted hot press, electro sinter forging, spark plasma sintering (SPS), etc. are now common sintering methods. Application of pressure causes a reduction in sintering temperature in pressure-assisted sintering technique, which improves the mechanical properties over conventional sintering [26,27]. Nauri Saheb stated that the spark plasma sintering technique was the best process for the Al 6061 alloy to achieve theoretical density and better mechanical properties [28]. In the current study, Al-TiB_2 composites were fabricated and effectively solid-state sintered at low pressure (30 MPa) using the spark plasma sintering technique at 500 °C and 550 °C sintering temperature. The investigation of the microstructures, Ultimate Tensile Strength (UTS), hardness, and physical properties of Al-TiB_2 composites at 500 °C and 550 °C sintering temperature was carried out.

2. Materials and Methods

Aluminum alloy 6061 powder synthesized by the gas atomized method with a particle size ~100 µm (from Ampal Inc. Flemington, NJ, USA) was used as a matrix material and TiB_2 with a 10 µm particle size (Krish Met, Chennai, India) and density of 4.52 g/cm^3 was used as reinforcement (Tables 1 and 2). The Scanning Electron Microscopy morphology of the as-received powders is shown in Figure 1. The Al powder and 2.5%, 5%, 7.5%, and 10% wt% TiB_2 was mixed homogenously by ball milling machine without balls for 20 min. Spark plasma sintering (SPS) system (Model: DR. Sinter 21050 SPS furnace) was used for the sintering of the mixed powders. The sintering was carried out in an argon atmosphere at 500 °C and 550 °C with a heating rate of 100 °C/min. During the complete span of heating and sintering, the powder compact was subjected to a uniaxial pressure of 30 MPa. The relative density of the sintered samples was obtained from the relationship between theoretical density ($\rho_{theoretical}$) and actual density (ρ_{actual}). The equation for theoretical density is given as follows:

$$\rho_{theoratical} = \sum (\rho_i \times w_i) \quad (1)$$

where ρ_i is the theoretical density of the *ith* element and w_i is the weight fraction of the *ith* element.

Table 1. Powder characteristics of the as received Al-6061.

Metal	Al	Mg	Fe	Si	Cu	Mn	Cr	Ti	Zn	Others
% Composition	95.8–98.6	0.8–1.2	0.7	0.4–0.8	0.15–0.4	0.15	0.04–0.35	0.15	0.25	0.2

Table 2. TiB_2 powder properties.

Characteristics	TiB_2
Apparent Density (g/cm^3)	2.3
Tapped Density (g/cm^3)	3.2
Flow rate in s/50 g	21
Theoretical Density g/cm^3	4.52
Shape	Irregular
Purity	99.5%

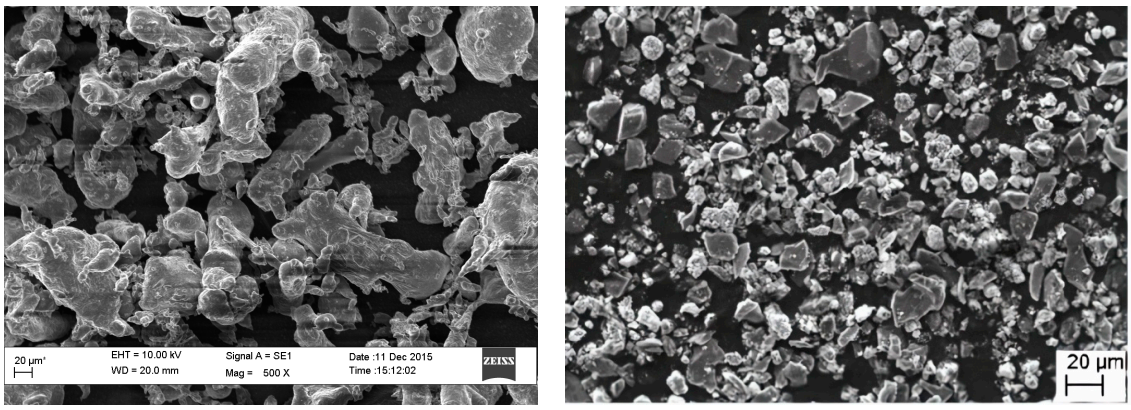

(**a**) (**b**)

Figure 1. Morphology of the as-received powders. (**a**) Al 6061, (**b**) TiB_2.

The Archimedes principle was used to evaluate the actual density of the samples, where w_1 and w_0 are the mass of the compacts in water and air, respectively, and ρ_0 is the water density.

$$\rho_{actual} = \frac{\rho_0 \cdot w_0}{w_0 - w_1} \tag{2}$$

For microscopic studies, initially, SiC sheets of various sizes (220, 400, 600, 800, 1000, and 1200) were used for polishing the sintered samples, and later, diamond paste (6 µm particles) was used for fine polishing. Keller's reagent (2 mL HF (48%) + 3 mL HCl + 5 mL HNO_3 + 190 mL distilled water) was used for etching on the polished samples to examine clear microstructures in an optical microscope (Leica DMS1000, Wetzlar, Germany) and scanning electron microscope (MODEL: ZEISS EVO180, Oberkochen, Germany). The hardness of sintered Al-TiB_2 composites was obtained using the Micro Vickers hardness tester (Leco Micro hardness testing machine LM248AT, St. Joseph, MI, USA). The indentation load applied on the sample was 0.5 kgf for a dwell period of ten seconds. The following formula gives the Micro Vickers hardness value.

$$\text{Vickers micro hardness value } = \frac{1.854P}{l^2} \tag{3}$$

where P is the exerted load in grams; and l is the mean length of d_1 and d_2 (diagonals).

Flat tensile samples, prepared as per the Metal Powder Industries Federation (MPIF) standards with a gauge length of 26 mm using the material testing machine (INSTRON 1195, Norwood, MA, USA) with the top-load of 20 kilos Newton at a strain rate of 3.3×10^{-4} per s in the beginning (cross-head velocity 0.5 mm/min), were used to measure the mechanical properties like ultimate tensile strength (UTS), yield strength, percentage elongation, and flexural strength.

3. Results and Discussion

3.1. Densification Behavior of Sintered Samples

Figure 2 lists the sintered density of Al-TiB_2 composites at 500 °C and 550 °C. As the concentration of TiB_2 in the Al-6061 matrix is increased, the sintered density also increases, and it is highest in 2.5% TiB_2 composite. The sintered density of the Al-6061 alloy was observed to be 85.12% at 500 °C, which increased up to 98.36% with 2.5% TiB_2 addition. Further increase in TiB_2 concentration up to 10% reduced the density to 92.2%. At 550 °C, a similar trend was observed with an increase in sintered density at 2.5% (99.81%), then decreased (92.2%) at 10% of TiB_2. The presence of TiB_2 particles restricts the expansion of pre-alloyed powder as the sintering takes place at solid-state conditions with a faster heating rate. As a result, the composites with a higher TiB_2 content had the least expansion in the initial stage of sintering, and later densification occurred due to a faster heating rate and the load displaced on the punch. A total of 2.5% TiB_2 powder in the Al matrix increased the density, but above 2.5%, TiB_2 sintered density was gradually decreased. The reason is that at 2.5%, TiB_2 concentration of reinforcement in the matrix uniformly distributed, but as the TiB_2 increased in the matrix, the reinforcement was not evenly distributed, and TiB_2 agglomeration and voids formed in the matrix. Increasing the sintering temperature from 500 °C to 550 °C with a fixed amount of TiB_2 improved the sintered density slightly with correspondingly lowering the porosity. This is due to the benefits of elevated temperature on diffusion rate, sinterability, and matrix reinforcement bonding [17,29–31].

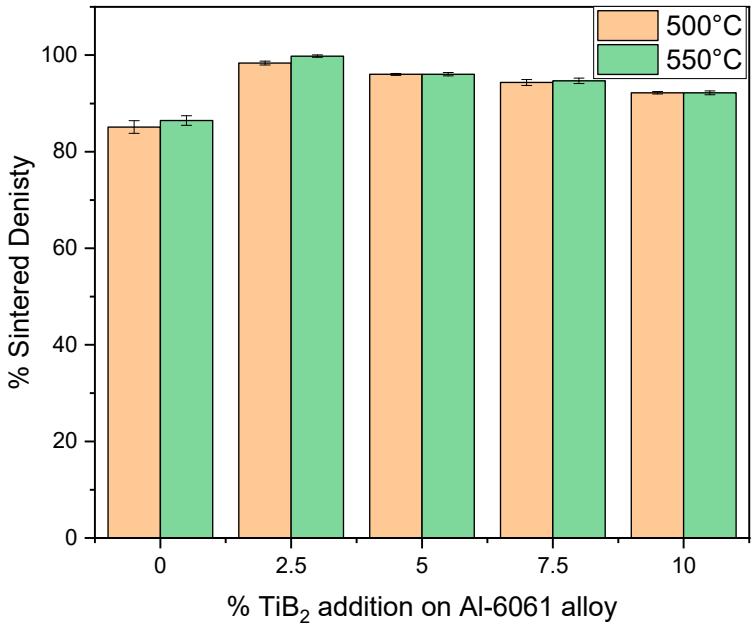

Figure 2. Sintered density of Al-TiB_2 composites.

3.2. Micro-Structural and SEM Analysis

SEM micrographs of the Al-TiB_2 compositions sintered at 500 °C and 550 °C are shown in Figure 3. From the micrographs, it was observed that temperature difference was showing the difference in the microstructure. The 500 °C sintered composite microstructures with a high area of light phase appeared when compared with the 550 °C sintered compacts, where the reason was that the temperature was not sufficient for the aluminum to fully pack around the TiB_2 particles. As the TiB_2 content increased in the matrix, TiB_2 particles restrict the Al-Al contacts and as a result, Al penetration in between the TiB_2 particles is restricted, which leads to the formation of the pores and slight reduction in the sintered density. Agglomerations (light phase) and porosity (dark phase) are crucial micro-structural

characteristics that can be observed in the SEM images [32]. This agglomeration might be the outcome of the localized distribution of powders, while blending due to the non-identical size and density of TiB_2 and Al-6061 [33]. It was observed from the micrographs that the aggregates of TiB_2 particles were dispersed in the aluminum matrix at grain boundaries forming clusters around the grain. An increase in TiB_2 content caused a decrease in uniformity and homogeneity [34]. This ultimately resulted in increasing agglomerations with an increase in the TiB_2 concentration in the Al-6061 composite. Porosity was decreased while the uniformity was increased by increasing the temperature from 500 °C to 550 °C due to an increase in sintered density. Compared with other (Mahesh Paidpilli [35], V. Jaya Prasad [36], Z.Sadeghian [20]) Al-TiB_2 composite microstructures, TiB_2 particles were not clearly visible in the current work microstructures.

3.3. Mechanical Properties

The micro Vickers hardness values of the Al alloy and Al-TiB_2 composites are displayed in Table 2. As Al is a soft metal and TiB_2, being a ceramic material with high hardness, this resulted in an increase in the hardness values of the metal matrix composites [37]. For Al at 500 °C, the hardness of pure Al-6061 was observed to be 65 $HV_{0.5}$, which increased to 76$HV_{0.5}$ with 2.5% TiB_2 addition. Furthermore, with an increase in TiB_2 concentration up to 10%, the hardness value declined to 68$HV_{0.5}$. At 550 °C, a similar trend was observed with an increase in hardness at 2.5% (77 $HV_{0.5}$) and then decreased up to 10% (72$HV_{0.5}$). As expected, the Vickers's hardness trends were analogous to that of sintered density. There was a substantial variation in the values of thermal expansion of Al-6061 (23.5×10^{-6} °C^{-1}) and TiB_2 (5.4×10^{-6} °C^{-1}), which causes residual stresses in the specimens during cooling. The strength of the MMC proliferates due to Orowan's mechanism, which allows the TiB_2 particulates to become obstacles to the migration of dislocations [38,39]. During SPS, hard and brittle TiB_2 particles restrict local rearrangement and plastic deformation of aluminum particles [35]. Furthermore, pre-alloyed 6061 Al powders are harder due to solid solution strengthening during processing, and the presence of the TiB_2 reinforcement particles in the matrix increases the hardness [40]. The tensile properties of composites are shown in Table 3. It was observed that the UTS of the composite increased from 112 MPa (Al-6061) to 314 MPa (Al-6061 + 10% TiB_2) at 500 °C and from 120 MPa (Al-6061) to 316 MPa (Al-6061 + 10% TiB_2) at 550 °C. The interaction between TiB_2 particles and dislocations contributes to the excellent tensile strength of the developed composites under load. The dislocation density increased in the matrix due to the mismatch of the coefficients of the thermal expansion of matrix, and reinforcement phases during the heating and cooling in the spark plasma sintering process [41]. The movement of dislocations under load was stopped by reinforcement particles and a hence substantial increase in tensile strength. As the TiB_2 volume increased in the matrix, the ductility was decreased due to the TiB_2 particles inhibiting the plastic flow [35]. A comparison (Table 4 shows a comparison of the tensile strength of the current work with other works with the other works (Selvaganesan M [42] Johny James. S [43], S. Suresh [44], V. Jaya Prasad [36] Fei Chen [45]) done on the Al alloy with different reinforcement ceramics with different manufacturing processes at different temperatures, showed that this solid state sintered Al-TiB_2 composite had better mechanical properties.

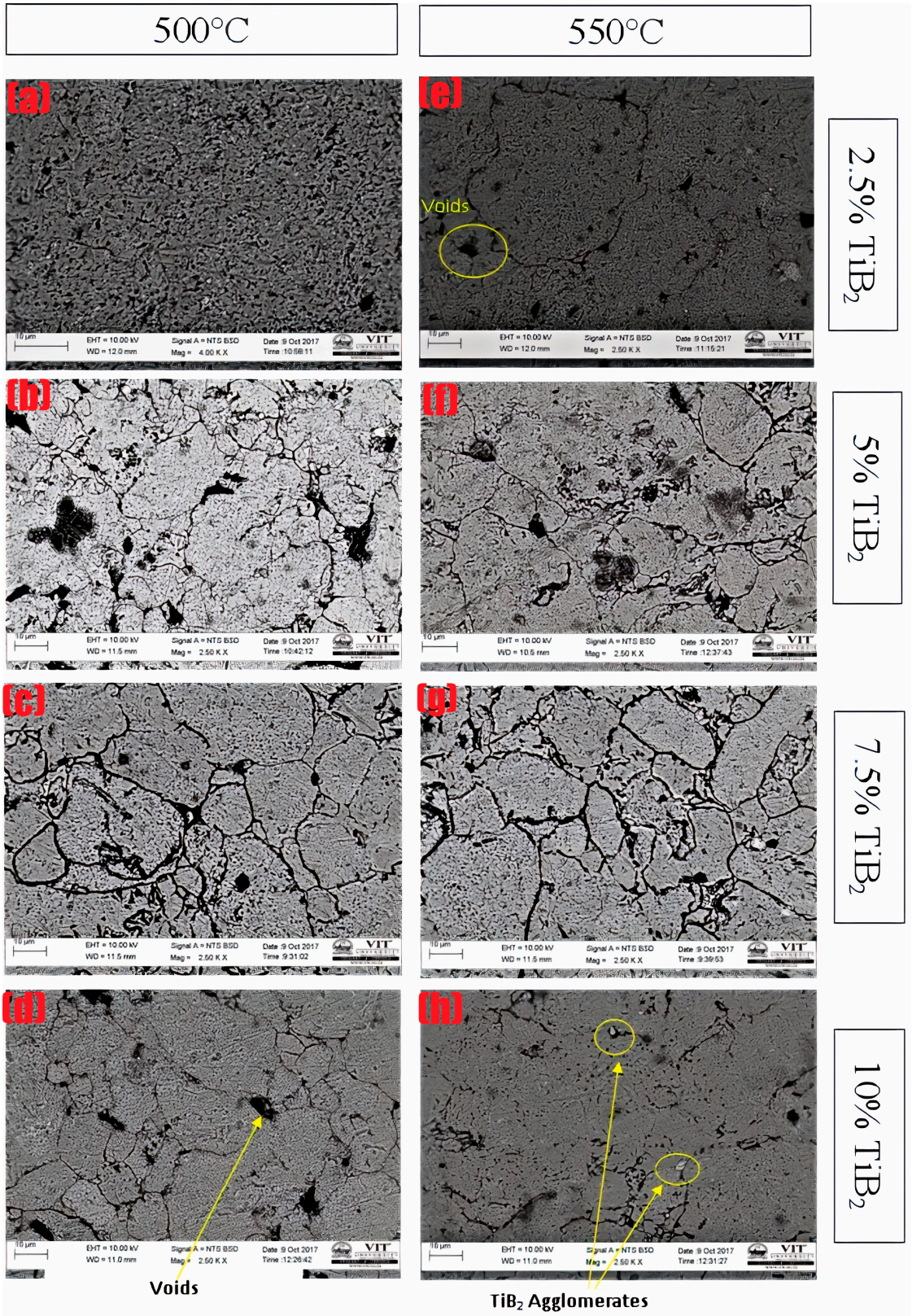

Figure 3. Scanning electron micrographs of spark plasma sintered Al-TiB_2 composites, 500 °C. (**a**) 2.5% TiB_2, (**b**) 5% TiB_2, (**c**) 7.5% TiB_2, (**d**) 10% TiB_2; 550 °C: (**e**) 2.5% TiB_2, (**f**) 5% TiB_2, (**g**) 7.5% TiB_2, (**h**) 10% TiB_2.

Table 3. Mechanical properties of the aluminum alloy.

wt% TiB_2 Composition	Temperature °C	Ultimate Tensile Strength (MPa)	Micro Vickers Hardness (HV)	Elongation (%)
Nil	500	112 ± 4	65 ± 2	12
	550	120 ± 7	68 ± 3	15
2.5	500	216 ± 5	76 ± 1	8
	550	223 ± 7	77 ± 2	3
5	500	254 ± 12	71 ± 2	4
	550	257 ± 5	74 ± 4	5
7.5	500	262 ± 6	68 ± 1	4
	550	282 ± 4	73 ± 2	7
10	500	314 ± 2	69 ± 3	9
	550	316 ± 1	75 ± 1	7

Table 4. Comparison of the tensile strength of Aluminium Metal Matrix Composite Works with the present work.

Authors	Composition	Tensile Strength	Fabrication Technique
Selvaganesan et al. (2013) [42]	Al-6061 alloy	178 MPa	Two Step Stir Casting
	Al-6061 + 3%TiB_2	198 MPa	
	Al-6061 + 6% TiB_2	207 MPa	
	Al-6061 + 9% TiB_2	219 MPa	
	Al-6061 + 12% TiB_2	210 MPa	
Johny James. et al. (2014) [43]	Al-6061 + 10%SiC + 0% TiB_2	150 MPa	Stir Casting
	Al-6061 + 10%SiC+2.5% TiB_2	54 MPa	
	Al-6061 + 10%SiC + 5% TiB_2	97 MPa	
Suresh et al. (2014) [44]	Al-6061 alloy	125 MPa	Stir Casting
	Al-6061 + 10% TiB_2	150 MPa	
	Al-6061 + 20% TiB_2	175 MPa	
	Al-6061 + 10% TiB_2 + 2%gGr	179 MPa	
	Al-6061 + 20% TiB_2 + 2%Gr	160 MPa	
Elvin Raju et al. (2018) [49]	Al-6061 + 3%SiC + 2% TiB_2	158.28 MPa	Stir Casting
	Al-6061 + 5%SiC + 5% TiB_2	155.90 MPa	
Hadian et al. (2019) [40]	Al/10 vol% of (TiC + TiB_2)	260 MPa	SPS-456 °C-50 MPa
	Al/20 vol% of (TiC + TiB_2)	342 MPa	
	Al/30 vol% of (TiC + TiB_2)	315 MPa	
	Al/40 vol% of (TiC + TiB_2)	298 MPa	
Current work	Al-6061 alloy	112 MPa	SPS-500 °C-30 MPa
	Al-6061 + 2.5% TiB_2	216 MPa	
	Al-6061 + 5% TiB_2	254 MPa	
	Al-6061 + 7.5% TiB_2	262 MPa	
	Al-6061 + 10% TiB_2	314 MPa	
Current work	Al-6061 alloy	120 MPa	SPS-550 °C-30 MPa
	Al-6061 + 2.5% TiB_2	223 MPa	
	Al-6061 + 5% TiB_2	257 MPa	
	Al-6061 + 7.5% TiB_2	282 MPa	
	Al-6061 + 10% TiB_2	316 MPa	

The fractography is shown in Figure 4. From the fractography analysis, the mix-mode of fracture can be clearly seen. It is inferred from the images that cup and cone type fractures occurred in the Al matrix, and the ductile mode of fracture occurred due to the coalescence of voids. No chemical bonds formed in between the Al and TiB_2 particles and so for each TiB_2 particle acting as the void.

When we applied a tensile load, the TiB_2 particle did not deform, the Al matrix around the TiB_2 particle was deformed, and a void was formed, which was attributed to the ductile fracture [46]. Whereas in the titanium diboride, a brittle fracture was seen due to it being a ceramic material. Micro-cracks are formed at the interfacial boundaries due to the residual stresses, which play a vital role in reducing the hardness values [47]. Generally, it can be inferred from the magnified view of fractographs that there were more fractured particles observed along the line made, intersecting the crack growth paths more than the debonded particles on the site. Plastic deformations in the sample proliferated while the sample was close to the sintering temperature (550 °C), which led to the dislocations of slip systems in the lattice structure [48].

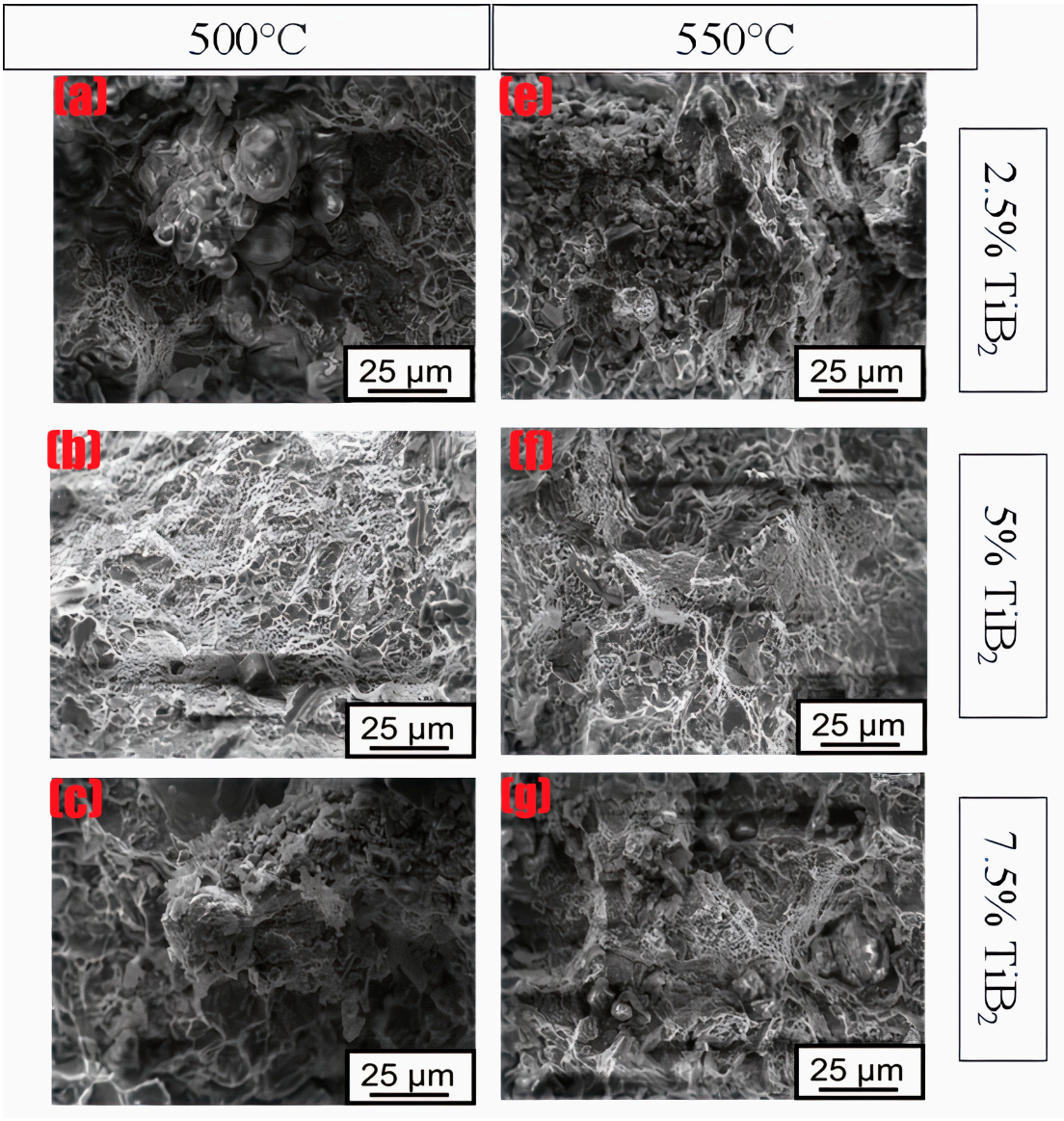

Figure 4. *Cont.*

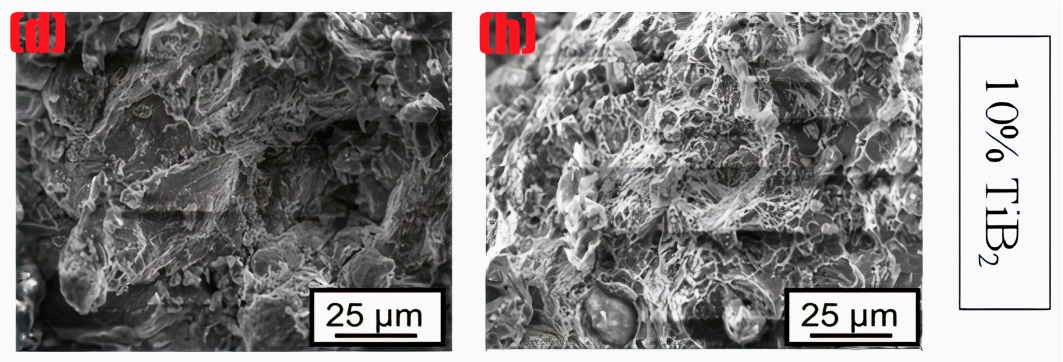

Figure 4. SEM Fractographs of Al-6061 at 500 °C: (**a**) 2.5% TiB_2, (**b**) 5% TiB_2, (**c**) 7.5% TiB_2, (**d**) 10%TiB_2; at 550 °C: (**e**) 2.5% TiB_2, (**f**) 5% TiB_2, (**g**) 7.5% TiB_2, (**h**) 10% TiB_2.

4. Conclusions

In this study, composites of Al-6061 and TiB_2 were fabricated by the solid state sintering successfully using the spark plasma sintering (SPS) technique at 500 °C and 550 °C under 30 MPa pressure. The main conclusions are the follows:

Sintered density and hardness values have shown similar trends. Sintered density increased by ~15.5% at 500 °C and ~15.4% at 550 °C with 2.5% TiB_2. Further increase in the content of TiB_2 decreased the sintered density at both temperatures. Hardness value increased by ~16% at 500 °C and there was a ~13% rise at 550 °C with 2.5% TiB_2 with respect to the Al-6061 alloy.

There was a significant increase in UTS with the addition of TiB_2 in the composite. The UTS increased gradually with the addition of TiB_2 at 500 °C as well as 550 °C.

From the SEM analysis, it was observed that the rate of agglomeration increased with the gradual increase in TiB_2 content. The degree of clustering of Al-TiB_2 nanoparticles is observed in the Al matrix, which is attributed to the difference in the densities between the matrix phase (2.7 g/cm^3) and the reinforcement phase (4.52 g/cm^3). The tendency of agglomeration at higher volume fractions of reinforcement arises because of the huge variation in the sizes of Al powder and TiB_2 powder particles. The nano-size powders tend to agglomerate at the interstitial sites between the Al powders during mixing and compaction.

There exist extensive equiaxed dimples on the fracture surface of Al-6061 alloy indicating the occurrence of large plastic deformation precisely before the failure. The development of micro-cracks is initiated under the local three-dimensional state of stress and propagates by increasing tensile load. Finally, these micro-cracks coalesce and reach a critical size, leading to the fracture of the sample.

Using spark plasma sintering, the sintered density of 99.8% at 2.5% addition of TiB_2 was achieved and was also corroborated by a Vickers hardness of 77 HV, which was the maximum.

It was found that even without reaching the liquid phase sintering temperature of the Al-6061 alloy (~600 °C), the samples attained 99.8% density at 550 °C with the addition of 2.5wt% TiB_2.

The unprecedented stiffness (2.5%, before ductile failure) was attained within the solid state sintering temperature.

The decrease in elongation with an increase in TiB_2 reinforcement shows that the dislocation density increased in the matrix and TiB_2 hindered the dislocation motion.

Author Contributions: Methodology, A.R.A.; experiment, M.S.; analysis, A.R.A., M.S., A.M., S.A., A.K., D.K.A. and C.-P.J.; writing—original draft preparation, A.R.A.; writing—review and editing, A.R.A. and C.-P.J. All authors have read and agreed to the published version of the manuscript.

Funding: The authors would like to acknowledge the Ministry of Science and Technology of the Republic of China (Taiwan) under grants MOST 109-2221-E-194-011-MY2 and MOST 107-2221-E-194-024-MY3.

Conflicts of Interest: The authors declare no conflict of interest.

References

1. Kaczmar, J.W.; Pietrzak, K.; Włosinski, W. The production and application of metal matrix composites. *J. Mater. Process. Technol.* **2000**, *106*, 58–67. [CrossRef]
2. Torralba, J.M.; daCosta, C.E.; Velasco, F. P/M aluminum matrix composites: An overview. *J. Mater. Process. Technol.* **2003**, *133*, 203–206. [CrossRef]
3. Ghasali, E.; Pakseresht, A.; Rahbari, A.; Eslami-shahed, H.; Alizadeh, M.; Ebadzadeh, T. Mechanical properties and microstructure characterization of spark plasma and conventional sintering of Al-SiC-TiC composites. *J. Alloy. Compd.* **2016**, *666*, 366–371. [CrossRef]
4. Shirvanimoghaddam, K.; Khayyam, H.; Abdizadeh, H.; Akbari, M.K.; Pakseresht, A.H.; Ghasali, E.; Naebe, M. Boron carbide reinforced aluminium matrix composite: Physical, mechanical characterization and mathematical modelling. *Mater. Sci. Eng. A* **2016**, *658*, 135–149. [CrossRef]
5. Ramesh, C.S.; Pramod, S.; Keshavamurthy, R. A study on microstructure and mechanical properties of Al 6061-TiB_2 in-situ composites. *Mater. Sci. Eng. A* **2011**, *528*, 4125–4132. [CrossRef]
6. Lekatou, A.; Karantzalis, A.E.; Evangelou, A.; Gousia, V.; Kaptay, G.; Gácsi, Z.; Baumli, P.; Simon, A. Aluminium reinforced by WC and TiC nanoparticles (ex-situ) and aluminide particles (in-situ): Microstructure, wear and corrosion behavior. *Mater. Des.* **2015**, *65*, 1121–1135. [CrossRef]
7. Toptan, F.; Kilicarslan, A.; Karaaslan, A.; Cigdem, M.; Kerti, I. Processing and microstructural characterisation of AA 1070 and AA 6063 matrix B_4Cp reinforced composites. *Mater. Des.* **2010**, *31*, S87–S91. [CrossRef]
8. Peng, L.M.; Li, Z.; Li, H.; Wang, J.H.; Gong, M. Microstructural characterization and mechanical properties of TiAl-$Al_2Ti_4C_2$-Al_2O_3-TiC in situ composites by hot-press-aided reaction synthesis. *J. Alloy. Compd.* **2006**, *414*, 100–106. [CrossRef]
9. Shirvanimoghaddam, K.; Khayyam, H.; Abdizadeh, H.; Akbari, M.K.; Pakseresht, A.H.; Abdi, F.; Abbasi, A.; Naebe, M. Effect of B_4C, TiB_2 and $ZrSiO_4$ ceramic particles on mechanical properties of aluminium matrix composites: Experimental investigation and predictive modelling. *Ceram. Int.* **2016**, *42*, 6206–6220. [CrossRef]
10. Casati, R.; Vedani, M. Metal matrix composites reinforced by nano-particles da review. *Metals* **2014**, *4*, 65–83. [CrossRef]
11. Shyu, R.F.; Ho, C.T. In situ reacted titanium carbide-reinforced aluminum alloys composite. *J. Mater. Process. Technol.* **2006**, *171*, 411–416. [CrossRef]
12. Rajabi, A.; Ghazali, M.J.; Daud, A.R. Chemical composition, microstructure and sintering temperature modifications on mechanical properties of TiC-based cermet—A review. *Mater. Des.* **2015**, *67*, 95–106. [CrossRef]
13. Yao, Y.T.; Chen, L.Q. B4C/Al Composites Processed by Metal-assisted Pressureless Infiltration Technique and its Characterization. *Mater. Manuf. Process.* **2016**, *31*, 1286–1291. [CrossRef]
14. Hu, Q.; Zhao, H.; Li, F. Effects of Manufacturing Processes on Microstructure and Properties of Al/A356-B4C Composites. *Mater. Manuf. Process.* **2016**, *31*, 1292–1300. [CrossRef]
15. Asano, K. Preparation of Alumina Fiber-Reinforced Aluminum by Squeeze Casting and Their Machinability. *Mater. Manuf. Process.* **2015**, *30*, 1312–1316. [CrossRef]
16. Singh, L.K.; Maiti, A.; Maurya, R.; Laha, T. Al Alloy Nanocomposite Reinforced with Physically Functionalized Carbon Nanotubes Synthesized via Spark Plasma Sintering. *Mater. Manuf. Process.* **2016**, *31*, 733–738. [CrossRef]
17. Munro, R.G. Material properties of titanium diboride. *J. Res. Natl. Inst. Stand. Technol.* **2000**, *105*, 709. [CrossRef]
18. Askarpour, M.; Sadeghian, Z.; Reihanian, M. Role of powder preparation route on microstructure poperties of Al-TiB_2 composites fabricated by accumulative roll bonding (ARB). *Mater. Sci. Eng. A* **2016**, *677*, 400–410. [CrossRef]
19. Singh, R.P.; Gupta, G.K.; Paliwal, M. Synthesis, Consolidation and Modelling Study of AA2014-TiB2 Composite Prepared by Powder Metallurgy (P/M) Method. In *Materials Science Forum*; Trans Tech Publications Ltd.: Stafa-Zurich, Switzerland, 2018; Volume 928, pp. 45–50.
20. Sadeghian, Z.; Lotfi, B.; Enayati, M.H.; Beiss, P. Microstructural and mechanical evaluation of Al–TiB_2 nanostructured composite fabricated by mechanical alloying. *J. Alloy. Compd.* **2011**, *509*, 7758–7763. [CrossRef]

21. Sadeghian, Z.; Enayati, M.H.; Beiss, P. Characterisation of in situ Al–TiB_2 nanocomposite powder synthesised by mechanical alloying. *Powder Metall.* **2011**, *54*, 46–49. [CrossRef]
22. Suresh, S.; Moorthi, N.S.V.; Vettivel, S.C.; Selvakumar, N. Mechanical behavior and wear prediction of stir cast Al-TiB_2 composites using response surface methodology. *Mater. Des.* **2014**, *59*, 383–396. [CrossRef]
23. Narimani, M.; Lotfi, B.; Sadeghian, Z. Investigating the microstructure and mechanical properties of Al-TiB_2 composite fabricated by Friction Stir Processing (FSP). *Mater. Sci. Eng. A* **2016**, *673*, 436–442. [CrossRef]
24. Vivekananda, A.S.; Prabu, S.B. Wear Behaviour of in Situ Al/TiB_2 Composite: Influence of the Microstructural Instability. *Tribol. Lett.* **2018**, *66*, 41. [CrossRef]
25. Vivekananda, A.S.; Prabu, S.B.; Paskaramoorthy, R. Combined effect of process parameters during aluminothermic reaction process on the microstructure and mechanical properties of in situ Al/TiB_2 composite. *J. Alloy. Compd.* **2018**, *735*, 619–634. [CrossRef]
26. Guillon, O.; Gonzalez-Julian, J.; Dargatz, B.; Kessel, T.; Schierning, G.; Räthel, J.; Herrmann, M. Field-assisted sintering technology/spark plasma sintering: Mechanisms, materials, and technology developments. *Adv. Eng. Mater.* **2014**, *16*, 830–849.
27. Suarez, M.; Fern_andez, A.; Men_endez, J.L.; Torrecillas, R.; Kessel, H.U.; Hennicke, J.; Kirchner, R.; Kessel, T. Challenges and opportunities for spark plasma sintering: A key technology for a new generation of materials. *BurcuErtug: Sinter. Appl.* **2013**, *13*, 320–328.
28. Saheb, N. Spark plasma and microwave sintering of Al6061 and Al2124 alloys. *Int. J. Miner. Metall. Mater.* **2013**, *20*, 152–159. [CrossRef]
29. DeGarmo, E.P.; Black, J.T.; Kohser, R.A. Powder Metallurgy. In *DeGarmo's Materials and Processes in Manufacturing*; John Wiley & Sons, Inc.: Hoboken, NJ, USA, 2012; Chapter 18; pp. 481–506.
30. Torizuka, S.; Sato, K.; Nishio, H.; Kishi, T. Effect of SiC on Interfacial Reaction and Sintering Mechanism of TiB_2. *J. Am. Ceram. Soc.* **1995**, *78*, 1606–1610. [CrossRef]
31. Park, J.H.; Koh, Y.H.; Kim, H.E.; Hwang, C.S. Densification and Mechanical Properties of Titanium Diboride with Silicon Nitride as a Sintering Aid. *J. Am. Ceram. Soc.* **1999**, *82*, 3037–3042. [CrossRef]
32. Baghchesara, M.A.; Abdizadeh, H.; Baharvandi, H.R. Production and microstructural investigation of Al-nano TiB_2 composite produced by powder metallurgy technique. *Int. J. Nano Dimens.* **2014**, *5*, 563–568.
33. Stone, I.C.; Tsakiropoulos, P. Characterization of spatial distribution of reinforcement in powder metallurgy route Al/SiCp metal matrix composites Part 1—Techniques based on microstructure. *Mater. Sci. Technol.* **1995**, *11*, 213–221. [CrossRef]
34. Abdizadeh, H.; Ashuri, M.; Moghadam, P.T.; Nouribahadory, A.; Baharvandi, H.R. Improvement in physical and mechanical properties of aluminum/zircon composites fabricated by powder metallurgy method. *Mater. Des.* **2011**, *32*, 4417–4423. [CrossRef]
35. Paidpilli, M.; Gupta, G.K.; Upadhyaya, A. Effect of matrix powder and reinforcement content on tribological behavior of particulate 6061Al-TiB_2 composites. *J. Compos. Mater.* **2019**, *53*, 1181–1195. [CrossRef]
36. Prasad, V.J.; Rao, K.N.; Babu, N.K. Mechanical and tribological characterization of aluminum metal matrix composite reinforced with micro ceramic particles (TiB_2/SiC). *Mater. Today Proc.* **2020**, *23*, 637–641. [CrossRef]
37. Charles, S.; Arunachalam, V.P. Effect of particle inclusion on the mechanical properties of composites fabricated by liquid metallurgy. *Indian J. Eng. Mater. Sci.* **2003**, *10*, 301–305.
38. Chen, D.; Wang, M.L.; Zhang, Y.J.; Li, X.F.; Chen, Z.; Ma, N.H.; Wang, H.W. Microstructure and mechanical properties of TiB_2/2219 composites. *Mater. Res. Innov.* **2014**, *18*, S4-514–S4-518. [CrossRef]
39. Lü, L.; Lai, M.O.; Su, Y.; Teo, H.L.; Feng, C.F. In situ TiB_2 reinforced Al alloy composites. *Scr. Matern.* **2001**, *45*, 1017–1023. [CrossRef]
40. Hadian, M.; Shahrajabian, H.; Rafiei, M. Mechanical properties and microstructure of Al/(TiC + TiB_2) composite fabricated by spark plasma sintering. *Ceram. Int.* **2019**, *45*, 12088–12092. [CrossRef]
41. Jerome, S.; Ravisankar, B.; Mahato, P.K.; Natarajan, S. Synthesis and Evaluation of Mechanical and High Temperature Tribological Properties of in-Situ Al-TiC Compo-Sites. *Tribol. Int.* **2010**, *43*, 2029–2036. [CrossRef]
42. Selvaganesan, M.; Suresh, S. Production and Characterization of Al 6061-TiB_2 Metal Matrix Composites. *Int. J. Eng. Res. Technol.* **2013**, *2*, 3154–3159.
43. James, S.J.; Venkatesan, K.; Kuppan, P.; Ramanujam, R. Hybrid aluminium metal matrix composite reinforced with SiC and TiB_2. *Procedia Eng.* **2014**, *97*, 1018–1026. [CrossRef]

44. Suresh, S.; Moorthi, N.; Prema, C.E. Tribological and mechanical behavior study of Al6061-TiB_2 metal matrix composites using stir casting. In *Advanced Materials Research*; Trans Tech Publications Ltd.: Stafa-Zurich, Switzerland, 2014; Volume 984, pp. 200–206.
45. Chen, F.; Chen, Z.; Mao, F.; Wang, T.; Cao, Z. TiB_2 reinforced aluminum based in situ composites fabricated by stir casting. *Mater. Sci. Eng. A* **2015**, *625*, 357–368. [CrossRef]
46. Priel, E.; Navi, N.U.; Mittelman, B.; Trabelsi, N.; Levi, M.; Kalabukhov, S.; Hayun, S. Cold Forming of Al-TiB_2 Composites Fabricated by SPS: A Computational Experimental Study. *Materials* **2020**, *13*, 3456. [CrossRef] [PubMed]
47. Alavi, S.H.; Baharvandi, H.R.; Abdizadeh, H. Densification and Mechanical Properties of TiB_2-sic Nanocomposite with Silicon Carbaid as a Sintering Aid. *Int. J. Mod. Phys. Conf. Ser.* **2012**, *5*, 598–606. [CrossRef]
48. Tan, A.; Teng, J.; Zeng, X.; Fu, D.; Zhang, H. Fabrication of aluminium matrix hybrid composites reinforced with SiC microparticles and TiB_2 nanoparticles by powder metallurgy. *Powder Metall.* **2017**, *60*, 66–72. [CrossRef]
49. Chevvakula, E.R.; Kumar, P.Y.; Sivananthan, S.; Vijayaganapathy, D. Investigation of Mechanical Properties for Al-Sic-TiB_2 Metal Matrix Composite. *Int. J. Pure Appl. Math.* **2018**, *118*, 24.